Office of Naval Research
Department of the Navy
Contract Nonr-220(41)

THE WALL EFFECT IN CAVITY FLOW

by

Daniel K. Ai

and

Z. L. Harrison

Hydrodynamics Laboratory
Karman Laboratory of Fluid Mechanics and Jet Propulsion
California Institute of Technology
Pasadena, California

Report No. 111.3

Approved by: T. Y. Wu

April 1965

ABSTRACT

A non-linear theory for the calculation of the flow field of an oblique flat plate under blockage condition is given using the techniques of integral equations. Numerical results are obtained with the aid of a high speed digital computer for the plate situated mid-channel at values of the angle of attack from 5° to 90° and the channel width-chord ratio from 3 to 20. Also obtained are results for the plate situated at two different off-center positions for a channel width-chord ratio 5 and angles of attack less than 30°.

NOMENCLATURE

A	=	leading edge of the plate; origin of the coordinate system.
B	=	trailing edge of the plate; $x = 1$.
C	=	scale factor.
C_D	=	drag coefficient.
C_L	=	lift coefficient.
D	=	stagnation point on the plate.
F_D	=	drag force.
f	=	complex potential.
H_A	=	normal distance from A to the upper channel wall.
H_1, H_2	=	widths of the flow above and below the dividing streamline at upstream infinity.
h_1, h_2	=	widths of the flow above and below the cavity at downstream infinity.
I	=	flow at upstream infinity.
J	=	flow at downstream infinity between the upper cavity and channel wall.
K	=	flow at downstream infinity between the lower channel and cavity wall.
k_o, k_1, k_2	=	parameters in the transformation.
p_∞	=	free stream pressure.
p_c	=	cavity pressure.
U, V	=	uniform up- and downstream velocities respectively.
W	=	channel width $= H_1 + H_2$.
w	=	complex velocity.
z	=	$x + iy$, the physical plane.
α	=	angle of attack.
σ	=	$(p_\infty - p_c)/\frac{1}{2} \rho U^2$, cavitation number.
ρ	=	density of the liquid.
θ	=	direction of the flow.

Introduction

The two-dimensional cavity theory of an unbounded fluid, with the recently published works[1], [2] on the non-linear solution of bodies of general shape, can be considered a well established field. For an experimentalist who has to perform the tests, however, the existing theories cannot always be applied directly and have to be modified mainly because the flow one creates for experiment is often bounded by different types of boundaries. These boundaries can be free surfaces of constant pressure if the equipment in use is a jet, rigid walls if it is a water tunnel, or both if it is a free surface channel. The essential problem is to determine the effect of the boundaries. In the past, many papers have been published on this problem. A small portion of these are listed here as references[3], [4], [5], [6]. We shall not repeat what they have done since these references are available and well known. This paper also deals with this problem, but the interest is focused only on the unsymmetric flow for arbitrary angle of attack and the boundaries considered are rigid walls. In a subsequent report, we shall treat the cases of the free jet and the free surface channel.

It is a well known fact that the cavity length behind a body depends essentially on σ, an important parameter known as the cavitation number and defined as

$$\sigma = (p_\infty - p_c)/\tfrac{1}{2}\rho U^2 . \qquad (1)$$

Here p_∞ is the free stream pressure, U the free stream velocity, and p_c is the cavity pressure presumably nearly constant. In general, the length would increase as σ decreases and with the presence of free surfaces, e.g. in a jet, σ would become zero when the length approaches infinity. However, this phenomenon is not observed in a water tunnel with rigid walls. In this case σ would reach a finite positive limit σ_c as the cavity length increases indefinitely hence cavitation numbers below σ_c are not attainable. Thus not all cavity flow conditions can be modeled in a water tunnel. The phenomenon corresponding to $\sigma = \sigma_c$ in a water tunnel is called blockage or choking and the determination of σ_c is therefore one of the central problems in water tunnel testing of cavity flows.

In this paper, the two-dimensional non-linear theory of a choked unsymmetrical flow over a flat plate at an arbitrary angle of attack is worked out using the techniques of integral equations. Numerical results are obtained on a high speed digital computer (IBM 7094).

Formulation of the problem and preliminary calculations.

Consider the idealized cavity flow in a water tunnel with rigid walls, depicted in Fig. 1. We assume a uniform upstream flow with velocity U, and a uniform downstream velocity V as the cavity, which has a stationary interface, approaches its maximum cross-section. The flat plate, set at an arbitrary angle of attack, can be located anywhere in the tunnel and the stream after impinging on the frontal side of the plate separates smoothly at both its leading and trailing edges. The plate is of length unity or one may say all dimensions are normalized by the chord. The coordinate axes are set normal and parallel to the plate with the origin at the leading edge.

If we call $\overline{w}$, the velocity vector, with magnitude $|w|$ and direction θ, $\overline{w} = |w| e^{i\theta}$, then in our coordinate system, the uniform velocities at up- and downstream infinities are $U e^{i\alpha}$ and $V e^{i\alpha}$ respectively.

The boundary conditions for the problem are:

$$\theta = \alpha, \quad \text{on the channel walls}$$
$$\theta = 0, \quad \text{on the plate from D to B}$$
$$\theta = \pi, \quad \text{on the plate from D to A}$$
$$|w| = V, \quad \text{on the cavity walls.}$$

The force coefficients at the choking condition can be obtained from momentum consideration in terms of the channel width, the angle of attack and the critical cavitation number;

$$\rho V^2 (h_1 + h_2) - \rho U^2 W = (p_\infty - p_c) W - F_D \tag{2}$$

where F_D is the drag, by conservation of volume, $V(h_1 + h_2) = WU$ and by definition $\sigma^* = (p_\infty - p_c)/\frac{1}{2}\rho U^2$. Substituting

$$F_D = (p_\infty - p_c) W + \rho U^2 W - \rho VUW \tag{3}$$

---

* The subscript is dropped since the cavitation number we refer to from now on is always the choked one.

and the drag coefficient is

$$C_D = \frac{2F_D}{\rho U^2 A^+} = 2W\left[(1 + \frac{\sigma}{2}) - \sqrt{1 + \sigma}\right]. \tag{4}$$

A^+, the area per unit span, is equal to one for a plate of unit length. The lift coefficient is

$$C_L = C_D \cot \alpha. \tag{5}$$

Theory

Assuming the flow to be irrotational, there exists a complex potential $f = \varphi + i\psi$. The flow field in the f-plane is shown in Fig. 2. The two channel walls are represented by the streamlines ψ_1 and $-\psi_2$ while the dividing streamline coincides with the negative φ-axis. The stagnation point D is chosen as the origin and the cut along the positive φ-axis represents the two branches of the streamline split at D. The leading and trailing edges of the plate are located somewhere on the upper and lower branches respectively. With reference to Fig. 1, the values of ψ_1 and ψ_2 are given as

$$\begin{aligned} \psi_1 &= UH_1 = Vh_1 \\ \psi_2 &= UH_2 = Vh_2. \end{aligned} \tag{6}$$

We proceed to solve the problem by introducing a new variable Ω, defined by

$$\begin{aligned} \Omega &= \log \frac{V}{w} = \tau + i\theta \\ \tau &= \log \frac{V}{|w|}, \quad \theta = -\arg w. \end{aligned} \tag{7}$$

The choice of using Ω as the dependent variable for the problem is suggested by the existing boundary conditions.

The flow fields in the f and the Ω-planes are to be connected through a parametric variable $\zeta = \xi + i\eta$. Consider the transformation

$$\frac{df}{d\zeta} = \frac{C}{(\zeta - k_o)(\zeta - k_1)(\zeta - k_2)} \tag{8a}$$

or

$$f(\zeta) = \frac{1}{\pi}\left[(h_1 + h_2)\log(\zeta - k_o) - h_1 \log(\zeta - k_1) - h_2 \log(\zeta - k_2)\right]. \tag{8b}$$

The flow in the f-plane is mapped into the upper half ζ-plane with the boundaries on the real ζ or ξ-axis as shown in Fig. 3. The upstream I behaves like a source at $\xi = k_o$ while the downstreams J and K behave like sinks at $\xi = k_1$ and k_2 respectively. The net strength of these singularities is certainly zero. The jump conditions on the f-plane further furnish the relations;

$$h_1 = \frac{-\pi C}{V} \frac{1}{(k_2 - k_1)(k_o - k_1)} \tag{9}$$

and

$$h_2 = \frac{-\pi C}{V} \frac{1}{(k_2 - k_1)(k_2 - k_o)} \quad . \tag{10}$$

Combining Eqs. (9) and (10) yields the ratio

$$\frac{h_1}{h_2} = \frac{k_2 - k_o}{k_o - k_1} \quad . \tag{11}$$

The constant C is a scale factor to be determined later in the theory.

Ω has the following values along the ξ-axis and $\eta = 0_+$.

$$\begin{aligned} &\text{Im}\,\Omega = \pi, && \xi < -1 \\ &\text{Im}\,\Omega = 0, && \xi > 1 \\ &\text{Re}\,\Omega = 0, && -1 < \xi < k_1,\ k_2 < \xi < 1 \\ &\text{Im}\,\Omega = \alpha, && k_1 < \xi < k_2 . \end{aligned} \tag{12}$$

We further define

$$\Omega = \Omega_o + \Omega_1 , \tag{13}$$

where Ω_o is associated with the unbounded fluid. Ω is split up in this way to make the solution readily obtainable. The term Ω_1, which represents the effect of the walls, is added to the unbounded fluid transcendentally to maintain the total exact solution. When the channel width-chord ratio is very large, Ω_1 then can be considered merely as a perturbation of the unbounded flow.

With reference to Figures 4a and 4b, Ω_o has the form

$$\Omega_o = \cosh^{-1}\zeta = \log\left(\zeta + \sqrt{\zeta^2 - 1}\right). \tag{14}$$

Along the ξ-axis,

$$\begin{aligned} &\text{Im}\,\Omega_o = \pi, && \xi < -1 \\ &\text{Im}\,\Omega_o = 0, && \xi > 1 \\ &\text{Re}\,\Omega_o = 0, && -1 < \xi < 1. \end{aligned} \tag{15}$$

For $|\xi| < 1$, Ω_o is given by

$$\text{Im}\,\Omega_o = \beta(\xi) = \arctan\left(\sqrt{1 - \xi^2}/\xi\right). \tag{16}$$

The remaining part, Ω_1 which is caused by the presence of the channel walls, then takes the boundary values;

$$\begin{aligned} &\text{Im}\,\Omega_1 = 0, && \xi < -1 \\ &\text{Im}\,\Omega_1 = 0, && \xi > 1 \\ &\text{Re}\,\Omega_1 = 0, && -1 < \xi < k_1, \quad k_2 < \xi < 1 \\ &\text{Im}\,\Omega_1 = \alpha - \beta(\xi), && k_1 < \xi < k_2. \end{aligned} \tag{17}$$

The boundary condition for Ω_1 on the ξ-axis is shown in Fig. 5. Three branch cuts appear on the ξ-axis; these are from $\xi = -\infty$ to $\xi = -1$, from $\xi = 1$ to $\xi = +\infty$ and from $\xi = k_1$ to $\xi = k_2$. The first two cuts represent the plate and the last one the channel walls in the z-plane.

We now have a boundary value problem involving the unknown function, $\Omega_1(\zeta)$, which can be formulated and solved as a Hilbert problem. By analytic continuation

$$\Omega_1(\bar{\zeta}) = -\bar{\Omega}_1(\zeta). \tag{18}$$

The region is extended to the lower half ζ-plane with the $\text{Re}\,\Omega_1$ odd and the $\text{Im}\,\Omega_1$ even with respect to the ξ-axis. We now introduce the auxiliary function

$$H(\zeta) = \frac{1}{\sqrt{(\zeta - k_1)(\zeta - k_2)(\zeta^2 - 1)}}, \tag{19}$$

which has the following properties;

i) $H(\zeta)$ has the proper branch cuts ($\zeta = -1$, k_1, k_2, and $+1$ are branch points).

ii) On the Re ζ axis:

$$\begin{aligned}
&\text{Im } H = 0, && -\infty < \xi < -1 \\
&\text{Re } H = 0, && -1 < \xi < k_1 \\
&\text{Re } H = -\frac{1}{\sqrt{(\xi - k_1)(k_2 - \xi)(1 - \xi^2)}}, \quad \text{Im } H = 0, && k_1 < \xi < k_2 \\
&\text{Re } H = 0, && k_2 < \xi < 1 \\
&\text{Im } H = 0, && 1 < \xi < \infty
\end{aligned}$$

A new function

$$G(\zeta) = \Omega_1(\zeta)\, H(\zeta)$$

is then formed which has on the Re ζ axis;

$$\begin{aligned}
&\text{Im } G = 0, && -\infty < \xi < k_1 \\
&\text{Im } G = -\frac{a - \beta(\xi)}{\sqrt{(\xi - k_1)(k_2 - \xi)(1 - \xi^2)}}, && k_1 < \xi_1 < k_2 \\
&\text{Im } G = 0, && k_2 < \xi < +\infty
\end{aligned}$$

With the aid of Plemelj's formula[7], the solution of the Hilbert problem is given immediately by

$$\Omega_1(\zeta) = -\frac{1}{\pi}\sqrt{(\zeta - k_1)(\zeta - k_2)(\zeta^2 - 1)} \int_{k_1}^{k_2} \frac{[a - \beta(t)]\, dt}{(t - \zeta)\sqrt{(t - k_1)(k_2 - t)(1 - t^2)}} \tag{20}$$

However, the constants k_1 and k_2 cannot be arbitrarily chosen for a fixed a because of a physical condition that must be imposed on the solution. Specifically, the solution Ω must behave locally like a stagnation flow at the stagnation point. In the ζ-plane, the stagnation point corresponds to $\zeta = \infty$. The local stagnation flow can be shown to behave like $\log \zeta$ as ζ approaches infinity; this behavior is already incorporated into the function Ω_o. We require, therefore that Ω_1 be finite at infinity. If Eq. (20) is expanded in inverse powers of ζ, this condition is seen to be given by the requirement that

$$\int_{k_1}^{k_2} \frac{\alpha - \beta(t)}{\sqrt{(t-k_1)(k_2-t)(1-t^2)}}\, dt = 0 . \tag{21}$$

Thus for a given value of α, Eq. (21) determines the relation between k_1 and k_2.

We are now able to determine σ from Ω_1 in Eq. (20). At upstream infinity in the physical plane, $|w| = U$ and $\zeta = k_o$.

$$\Omega_1 = \tau_1 = \log \frac{V}{U} = \frac{1}{\pi}\sqrt{(k_2 - k_o)(k_o - k_1)(1-k_o^2)} \int_{k_1}^{k_2} \frac{[\alpha - \beta(t)]\, dt}{(t-k_o)\sqrt{(t-k_1)(k_2-t)(1-t^2)}} . \tag{22}$$

From our previous discussion, $\sigma = V^2/U^2 - 1$, therefore Eq. (22) enables us to calculate σ when the integral on the right hand side is evaluated.

In order to complete the solution, we shall relate the geometry of the flow to the undetermined constants. Utilizing the definition of the complex velocity, we have the relation

$$dz = \frac{1}{w}\, df = \frac{1}{w}\, \frac{df}{d\zeta}\, d\zeta = \frac{1}{V}\, e^{\Omega(\zeta)}\, \frac{df}{d\zeta}\, d\zeta . \tag{23}$$

With the aid of Eqs. (8a), (13) and (14) and upon integration,

$$\int dz = \frac{C}{V} \int \frac{\zeta + \sqrt{\zeta^2 - 1}}{(\zeta - k_o)(\zeta - k_1)(\zeta - k_2)}\, e^{\Omega_1(\zeta)}\, d\zeta . \tag{24}$$

When we apply Eq. (24) along the plate from A to B, the normalized chord is obtained;

$$z_B - z_A = 1 = \frac{C}{V}\left[\int_{\infty}^{1} \frac{\xi + \sqrt{\xi^2 - 1}}{(\xi - k_o)(\xi - k_1)(\xi - k_2)}\, e^{\Omega_1(\xi)}\, d\xi - \int_{-\infty}^{-1} \frac{\xi - \sqrt{\xi^2 - 1}}{(\xi - k_o)(\xi - k_1)(\xi - k_2)}\, e^{\Omega_1(\xi)}\, d\xi\right]. \tag{25}$$

The first integral on the right hand side represents the distance from the stagnation point to the trailing edge, we therefore find the location of the stagnation point.

H_A, the height of A below the upper channel wall can be determined in a similar way. With reference again to Fig. 1,

$$H_A = h_1 + \mathrm{Im}\left[e^{-i\alpha}(z_J - z_A)\right]$$

$$= h_1 + \frac{C}{V}\,\mathrm{Im}\left[e^{-i\alpha}\int_{-1}^{k_1} \frac{e^{i\beta(\xi)}\, e^{\Omega_1(\xi)}}{(\xi - k_o)(\xi - k_1)(\xi - k_2)}\, d\xi\right]$$

or

$$= h_1 + \frac{C}{V}\int_{-1}^{k_1} \frac{\sin(\theta_1 + \beta - \alpha)}{(\xi - k_o)(\xi - k_1)(\xi - k_2)}\, d\xi, \qquad (26)$$

since Ω_1 is purely imaginary and equal to $i\theta_1$ in the interval $-1 \le \xi \le k_1$.

The channel width W is expressed through continuity as

$$W = (h_1 + h_2)\frac{V}{U} = \frac{(h_1 + h_2)}{\sqrt{1 + \sigma}}\,. \qquad (27)$$

Final Results.

We have applied the theory to calculate the case of a flat plate positioned mid-channel for various values of α and W. The range in α is from 5^o to 90^o and in W from 3 chords to 20 chords. We also obtained results for two off-center positions of the plate, $H_A = 1.0$ and 4.0 for $W = 5$ chords and values of α up to 30^o.

The lift coefficient, drag coefficient and choking cavitation number are plotted versus α for $W = 5$ chords and the plate in mid-channel in Fig. 6. The dash-dot curve in Fig. 6 is the lift coefficient given by Wu's unbounded fluid theory[1].

In Fig. 7, we show the enlarged portion of Fig. 6 for $\alpha \le 30^o$ with experimental values from Wade[8] corresponding to the choking σ determined by the present theory. Wade's experiment was performed with $W \approx 5$ and the experimental cavitation numbers were obtained from measured cavity pressure. Since it is difficult to operate the tunnel near choking condition, Wade was not able to obtain data at such low cavitation numbers: Therefore, we show values extrapolated from his data curves. One notices that all points are enveloped by the two theoretical curves.

Cohen, Sutherland and Tu[5] have worked out a linearized theory for a flat plate at small angles of attack and calculated σ for mid-channel position. However, their definition of mid-channel is different from ours as we define mid-channel when the center of the plate lies on the centerline while they locate the leading edge of the plate on the centerline. As a result, it is not possible to make a direct comparison between the two theories. For very small angles of attack, however, the discrepancy caused by the difference in definition becomes small and for $\alpha = 6^{\circ}$, $W = 5$, the present theory gives $\sigma = 0.133$, $C_L = 0.198$ for $H_A/(W-H_A) = 0.959$ and their theory gives $\sigma \approx 0.13$ and $C_L \approx 0.22$ for $H_A/(W-H_A) = 1$. The values of their calculations are read from Fig. 10 of Ref. 3, hence are only approximate.

Figure 8 shows the effect of plate position for $W = 5$ chords. In this figure C_L, C_D and σ are plotted versus α for $\alpha \leq 30^{\circ}$ and two values of H_A. The dashed curves are $H_A = 1.0$ and the solid ones are $H_A = 4.0$. As would be expected C_L, C_D and σ all increase as the plate is lowered in the channel.

We show C_L and σ versus α for $W = 8$ with experimental values from Parkin[9] in Fig. 9. Again the experimental cavitation numbers were obtained from measured cavity pressure, however, in this case only the data for $\alpha = 8^{\circ}$ and 10° were obtained from extrapolated curves.

Figures 10a and b show drag coefficient, C_D, and choking cavitation number, σ, versus channel width, W, for a flat plate located mid-channel. The range in angle of attack is 5° to 90° and in W from 3 to 20 chords. C_L may easily be obtained from Fig. 10a and Eq. (5) and therefore is not presented here.

In order to show the effect of the channel walls, we have plotted RC_D, the ratio of C_D bounded to C_D unbounded [1], ($RC_N = RC_L = RC_D$) versus the channel width W in Fig. 11. The curves are for the same values of α and W as Figs. 10a and b except that for $\alpha = 90^{\circ}$ RC_D is shown for W as low as 1.224. As would be expected when $W = 20$ there is very little wall effect and as the channel becomes smaller the ratio drops until the walls approach the plate where the ratio increases. This effect is shown for $\beta = 90^{\circ}$ where the ratio tends to infinity at $W = 1$.

The curve of RC_D for each α will have a similar asymptote at $W = \sin\alpha$.

In Fig. 12, we have shown the distance of the stagnation point from the leading edge as a function of α. At $\alpha = 15^\circ$, it is already difficult to tell the difference between the two points and at $\alpha = \frac{\pi}{2}$ the stagnation point is at mid-plate as one would expect.

ACKNOWLEDGMENT

This work is supported by the U. S. Office of Naval Research under Contract Nonr-220(41) at the California Institute of Technology. The authors also wish to express their sincere thanks to Professor T. Y. Wu for his suggestions and guidance in this problem, to Dr. D. P. Wang for the many helpful discussions they had, and to Miss C. Lin for the graphical works.

REFERENCES

1. Wu, T. Y., "A wake model for free-streamline flow theory. Part I. Fully and partially developed wake flows and cavity flows past an oblique flat plate", Journal of Fluid Mechanics, Vol. 13 part 2, pp. 161-181, 1962.

2. Wu, T. Y. and Wang, D. P., "A wake model for free-streamline flow theory, Part II, Cavity flows past obstacles of arbitrary Profile", California Institute of Technology, Hydrodynamics Laboratory Report No. 97.4, May 1963.

3. Cohen, H. and DiPrima, R. C., "Wall effects in cavitating flows", pp. 367-390, Aug. 25--29, 1958.

4. Birkhoff, G., Plesset, M. and Simmons, N., "Wall effects in cavity flow I", Quarterly of Applied Mathematics, Vol. VIII, No. 2, July 1950.

5. Cohen, H., Sutherland, C. C. and Tu, Yih-O, "Wall effects in cavitating hydrofoil flow", Journal of Ship Research, 3, (1957), pp. 31-40.

6. Gurevich, M. I., "Symmetrical cavitation flow around a flat plate situated between parallel walls", Bull. of Acad. of Sci, of USSR, No. 4(1946).

7. Mikhlin, S. G., "Integral equations", Pergamon Press, 1957.

8. Wade, R. B., "Water tunnel observations on the flow past a plano-convex hydrofoil", California Institute of Technology, Hydrodynamics Laboratory Report No. E-79.6, Feb. 1964.

9. Parkin, B. R., "Experiments on circular arc and flat plate hydrofoils in non-cavitating and full cavity flows", California Institute of Technology, Hydrodynamics Laboratory Report No. 47.6, Feb. 1956.

APPENDIX

Procedures for numerical computations

In a direct problem one would specify the channel width, W, and the location of the plate (of chord unity), H_A, for a given angle of attack, then calculate σ, h_1, h_2 and the force coefficients. However, in view of the form of our solution it is necessary to do the inverse problem of choosing the transformation parameters k_2, k_1, and k_o (the downstream conditions, h_1 and h_2, when the flow is choked) and calculating W and H_A. The values of h_1 and h_2 are related to the k's through the transformations in Eqs. (8a), (8b) and the jump conditions in Eqs. (9) and (10). The choice of k_2 defines the geometry so that the scaling factor, C, or more precisely, the ratio V/C is determined from Eq. (25).

Given a value of k_2, k_1 is easily determined by iteration of the integral condition of Eq. (21). The integral in this equation cannot be numerically integrated in its present form so we divide it into two integrals

$$\int_{k_1}^{k_2} \frac{\alpha-\beta(t)}{\sqrt{(t-k_1)(k_2-t)(1-t^2)}}\,dt = \int_{k_1}^{\frac{k_1+k_2}{2}} \frac{\alpha-\beta(t)}{\sqrt{(t-k_1)(k_2-t)(1-t^2)}}\,dt + \int_{\frac{k_1+k_2}{2}}^{k_2} \frac{\alpha-\beta(t)}{\sqrt{(t-k_1)(k_2-t)(1-t^2)}}\,dt; \tag{A-1}$$

make the transformations

$$p = x^2 + k_1 \qquad \text{in the first integral,}$$

$$s = k_2 - x^2 \qquad \text{in the second integral,}$$

and

$$x_o^2 = \tfrac{1}{2}(k_2 - k_1)$$

and Eq. (21) becomes

$$\int_0^{x_o} \frac{\alpha-\beta(p)}{p^2\sqrt{2x_o^2-x^2}}\,dx + \int_0^{x_o} \frac{\alpha-\beta(s)}{s^2\sqrt{2x_o^2-x^2}}\,dx = 0. \tag{A-2}$$

This integral iteration presents no problem since all calculations are preformed on a high speed digital computer (IBM 7094). We now can calculate the remaining transformation parameter, k_o, from the specified ratio h_2/h_1 and Eq. (11).

To aid in the trial and error solution of this problem the behavior of k_2 and k_1 for the plate in mid-channel are shown in Fig. A-1 and for the off center positions in Fig. A-2. The remaining parameter to be guessed is h_2/h_1 which may be approximated by $(W-H_A-\sin\alpha)/H_A$. For the mid-channel case this quantity is roughly unity.

The choking cavitation number, σ, the channel width, W, the drag coefficient, C_D, and the lift coefficient, C_L, are readily determined from Eqs. (22), (27), (4) and (5) respectively. The integral in Eq. (22) is treated in the same way as Eq. (21).

To determine H_A we must first evaluate the ratio V/C. From Eq. (25)

$$\frac{V}{C} = -\int_1^\infty \frac{\xi+\sqrt{\xi^2-1}}{(\xi-k_o)(\xi-k_1)(\xi-k_2)}\, e^{\Omega_1(\xi)}d\xi \; -\int_1^\infty \frac{\xi+\sqrt{\xi^2-1}}{(\xi+k_o)(\xi+k_1)(\xi+k_2)}\, e^{\Omega_1'(\xi)}\,d\xi, \qquad (A-3)$$

where $\Omega_1(\xi)$ is given in Eq. (20) and

$$\Omega_1'(\xi) = -\frac{1}{\pi}\sqrt{(\xi+k_1)(\xi+k_2)(\xi^2-1)}\int_{k_1}^{k_2}\frac{\alpha-\beta(t)}{(t+\xi)\sqrt{(t-k_1)(k_2-t)(1-t^2)}}\,dt. \qquad (A-4)$$

For numerical integration, it is more convenient to introduce the new integration variable $\tau = \xi^{-1}$. The first integral on the right hand side of Eq. (A-3) now may be written

$$\int_1^\infty \frac{\xi+\sqrt{\xi^2-1}}{(\xi-k_o)(\xi-k_1)(\xi-k_2)}\, e^{\Omega_1(\xi)}\,d\xi =$$

$$\int_o^{\tau_o} \frac{1+\sqrt{1-\tau^2}}{(1-k_o\tau)(1-k_1\tau)(1-k_2\tau)}\, e^{\Omega_1^\dagger}\,d\tau + \int_{\tau_o}^1 \frac{1+\sqrt{1-\tau^2}}{(1-k_o\tau)(1-k_1\tau)(1-k_2\tau)}\, e^{\Omega_1^*}\,d\tau, \qquad (A-5)$$

and the second integral

$$\int_1^\infty \frac{\xi + \sqrt{\xi^2 - 1}}{(\xi + k_0)(\xi + k_1)(\xi + k_2)} e^{\Omega_1'(\xi)} \, d\xi =$$

$$\int_0^{\tau_0} \frac{1 + \sqrt{1 - \tau^2}}{(1 + k_0\tau)(1 + k_1\tau)(1 + k_2\tau)} e^{\Omega_1'^{+}} \, d\tau + \int_{\tau_0}^{1} \frac{1 + \sqrt{1 - \tau^2}}{(1 + k_0\tau)(1 + k_1\tau)(1 + k_2\tau)} e^{\Omega_1'^{*}} \, d\tau, \quad \text{(A-6)}$$

where

$$\Omega_1^{+} = \frac{1}{\pi} \sqrt{(1 - k_1\tau)(1 - k_2\tau)(1 - \tau^2)} \left[g_1 + \tau g_2 + \tau^2 g_3 + \ldots + \tau^6 g_7 \right], \quad \text{(A-7)}$$

$$\Omega_1'^{+} = \frac{1}{\pi} \sqrt{(1 + k_1\tau)(1 + k_2\tau)(1 - \tau^2)} \left[g_1 - \tau g_2 + \tau^2 g_3 - \ldots + \tau^6 g_7 \right], \quad \text{(A-8)}$$

$$\Omega_1^{*} = \frac{1}{\pi\tau} \sqrt{(1 - k_1\tau)(1 - k_2\tau)(1 - \tau^2)} \int_{k_1}^{k_2} \frac{\alpha - \beta(t)}{(1 - t\tau)\sqrt{(t - k_1)(k_2 - t)(1 - t^2)}} \, dt, \quad \text{(A-9)}$$

$$\Omega_1'^{*} = -\frac{1}{\pi\tau} \sqrt{(1 + k_1\tau)(1 + k_2\tau)(1 - \tau^2)} \int_{k_1}^{k_2} \frac{\alpha - \beta(t)}{(1 + t\tau)\sqrt{(t - k_1)(k_2 - t)(1 - t^2)}} \, dt, \quad \text{(A-10)}$$

and

$$g_n = \int_{k_1}^{k_2} \frac{t^n [\alpha - \beta(t)] \, dt}{\sqrt{(t - k_1)(k_2 - t)(1 - t^2)}} . \quad \text{(A-11)}$$

Ω^{+} and Ω'^{+} are obtained from the power series expansion of τ and therefore are suitable for the calculation of small values of τ or large values of ξ. For a properly chosen τ_0, say $\tau_0 = 0.1$, a truncated series of seven terms is sufficient to give $\Omega_1^{+}(\tau_0)$ identical to $\Omega_1^{*}(\tau_0)$ to five significant figures.

The remaining quantity to be evaluated is the integral in Eq. (26)

$$\int_{k_1}^{k} \frac{\sin(\theta_1 + \beta - \alpha)}{(\xi - k_0)(\xi - k_1)(\xi - k_2)}\, d\xi .$$

Some analysis is needed before a straightforward numerical integration can be performed. One notices that the denominator of the integrand has a factor $(\xi - k_1)$ which causes the integral to be logarithmically singular unless the numerator also vanishes at the upper limit. It is therefore necessary to examine the behavior of the numerator as ξ approaches k_1. Let us study the behavior of

$$\theta_1 = \frac{1}{\pi} \sqrt{(k_1 - \xi)(k_2 - \xi)(1 - \xi^2)} \int_{k_1}^{k_2} \frac{\alpha - \beta(t)}{(t - \xi)\sqrt{(t - k_1)(k_2 - t)(1 - t^2)}}\, dt \qquad \text{(A-12)}$$

as ξ approaches k_1. We denote the regular part of the integrand in the neighborhood of $t = k_1$ as

$$F(t) = \frac{\alpha - \beta(t)}{\sqrt{(k_2 - t)(1 - t^2)}} . \qquad \text{(A-13)}$$

$F(t)$ has the Taylor expansion

$$F(t) = F(k_1) + F'(k_1)(t - k_1) + \frac{F''(k_1)}{2}(t - k_1)^2 + \ldots$$

where the coefficients $F(k_1)$, $F'(k_1)$ etc. are finite numbers which can be evaluated without any difficulty. If we now subtract from $F(t)$ the first terms of its Taylor expansion then add them on later, the integral in θ_1 can be written

$$\int_{k_1}^{k_2} \frac{[\alpha - \beta(t)]\, dt}{(t - \xi)\sqrt{(t - k_1)(k_2 - t)(1 - t^2)}} =$$

$$\int_{k_1}^{k_2} \frac{dt}{(t - \xi)\sqrt{t - k_1}} \left[F(t) - F(k_1) - F'(k_1)(t - k_1) - \frac{F''(k_1)}{2}(t - k_1)^2 \right]$$

$$+ F(k_1) \int_{k_1}^{k_2} \frac{(t - k_1)^{-\frac{1}{2}}}{t - \xi}\, dt + F'(k_1) \int_{k_1}^{k_2} \frac{(t - k_1)^{\frac{1}{2}}}{t - \xi}\, dt + \frac{F''(k_1)}{2} \int_{k_1}^{k_2} \frac{(t - k_1)^{\frac{3}{2}}}{t - \xi}\, dt. \qquad \text{(A-14)}$$

The integrand of the first integral of Eq. (A-14) is finite and tends to zero as t approaches k_1 because the terms in the bracket are of the order $(t-k_1)^3$. The remaining integrals of Eq. (A-14) are integrated in closed form:

$$\int_{k_1}^{k_2} \frac{1}{t-\xi}\frac{dt}{\sqrt{t-k_1}} = \frac{2}{\sqrt{k_1-\xi}}\left[\frac{\pi}{2} - \tan^{-1}\sqrt{\frac{k_1-\xi}{k_2-k_1}}\right]$$

$$\int_{k_1}^{k_2} \frac{\sqrt{t-k_1}}{t-\xi}\,dt = 2\sqrt{k_2-k_1} - 2\sqrt{k_1-\xi}\left[\frac{\pi}{2} - \tan^{-1}\sqrt{\frac{k_1-\xi}{k_2-k_1}}\right]$$

$$\int_{k_1}^{k_2} \frac{(t-k_1)^{\frac{3}{2}}}{t-\xi}\,dt = \frac{2}{3}(k_2-k_1)^{\frac{3}{2}} - 2(k_2-k_1)\sqrt{k_1-\xi} + 2(k_1-\xi)^{\frac{3}{2}}\left[\frac{\pi}{2} - \tan^{-1}\sqrt{\frac{k_1-\xi}{k_2-k_1}}\right].$$

From Eqs. (A-13) and (A-14) it can be shown that in the neighborhood of $\xi = k_1$, θ_1 has the asymptotic expression

$$\theta_1 = \alpha - \beta + M\sqrt{k_1-\xi} + O(k_1-\xi)$$

where

$$M = \frac{\sqrt{(k_2-k_1)(1-k_1^2)}}{\pi}\int_{k_1}^{k_2}\frac{dt}{(t-k_1)^{\frac{3}{2}}}\left[F(t) - F(k_1) - F'(k_1)(t-k_1) - \frac{F''(k_1)}{2}(t-k_1)^2\right]$$

$$- \frac{2}{\pi}\frac{\alpha-\beta(k_1)}{\sqrt{k_2-k_1}} + \frac{2F'(k_1)}{\pi}\sqrt{1-k_1^2}\,(k_2-k_1) + \frac{F''(k_1)}{3\pi}\sqrt{1-k_1^2}\,(k_2-k_1)^2. \qquad \text{(A-15)}$$

In our final form for numerical computation, the range of integration of the integral in Eq. (26) is split into two intervals;

$$\int_{-1}^{k_1} \frac{\sin(\theta_1 + \beta - \alpha)}{(\xi - k_0)(\xi - k_1)(\xi - k_2)}\, d\xi = \int_{-1}^{k_1 - \epsilon} \frac{\sin(\theta_1 + \beta - \alpha)}{(\xi - k_0)(\xi - k_1)(\xi - k_2)}\, d\xi + \int_{k_1 - \epsilon}^{k_1} \frac{(\theta_1 + \beta - \alpha)\, d\xi}{(\xi - k_0)(\xi - k_1)(\xi - k_2)}, \qquad \text{(A-16)}$$

where ϵ, small and positive, is chosen so that at $\xi = k_1 - \epsilon$, $\sin(\theta_1 + \beta - \alpha)$ can be safely approximated by $\theta_1 + \beta - \alpha$. If we replace θ_1, in the second integral of Eq. (A-16) by its asymptotic expression, Eq. (26) becomes

$$H_A = h_1 + \frac{C}{V}\left[\int_{-1}^{k_1 - \epsilon} \frac{\sin(\theta_1 + \beta - \alpha)}{(\xi - k_0)(\xi - k_1)(\xi - k_2)}\, d\xi - 2M \int_0^{\sqrt{\epsilon}} \frac{d\lambda}{(k_0 - \xi)(k_2 - \xi)} \right], \qquad \text{(A-17)}$$

where

$$\lambda^2 = k_1 - \xi$$

The integrals in Eq. (A-17) can be easily evaluated since their integrands are regular everywhere.

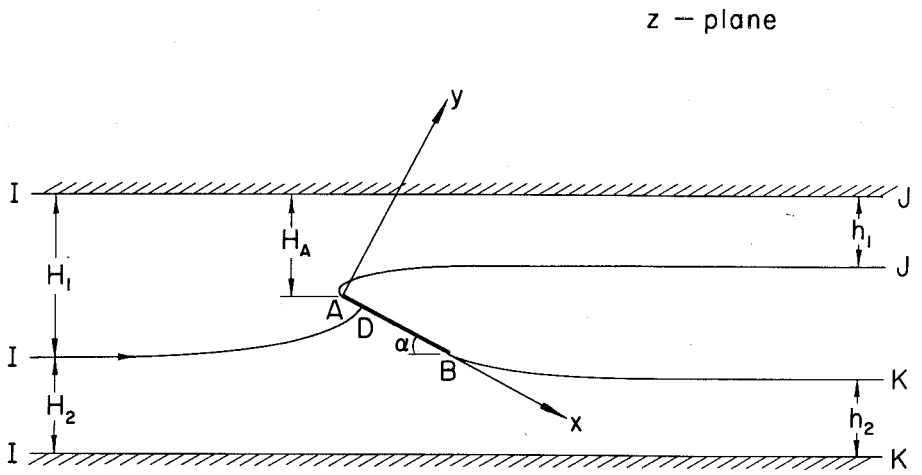

Fig. 1 Sketch showing a flat plate with an infinite cavity in a water tunnel.

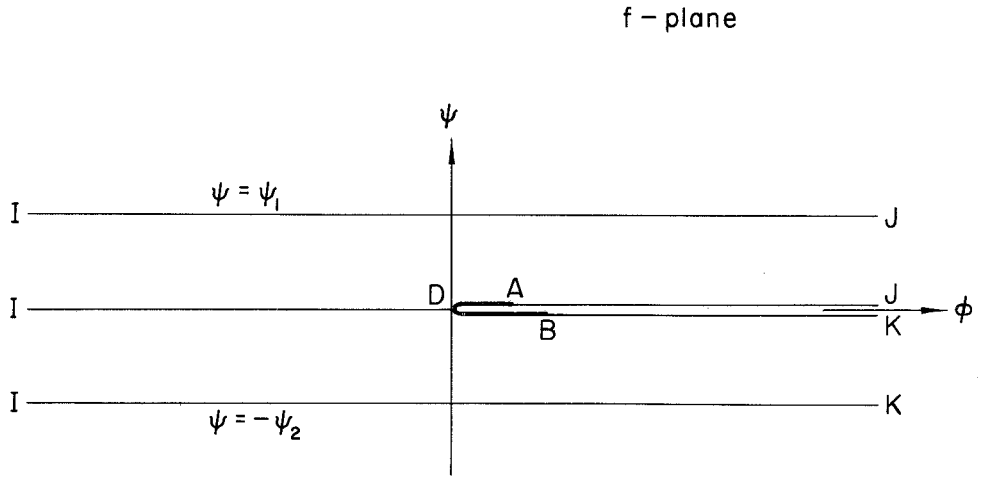

Fig. 2 The complex potential plane of the flow.

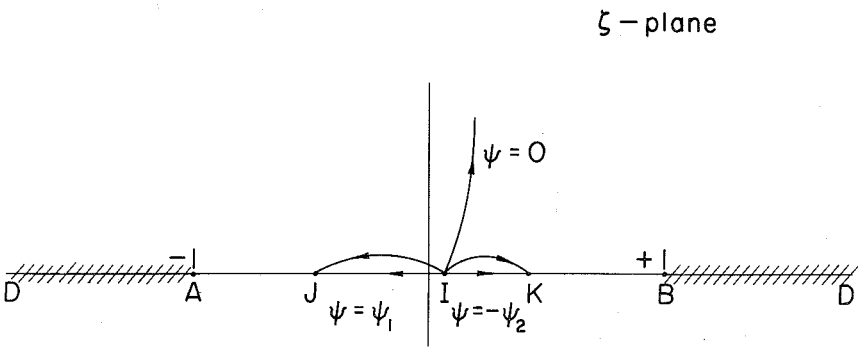

Fig. 3 The parametric ζ-plane.

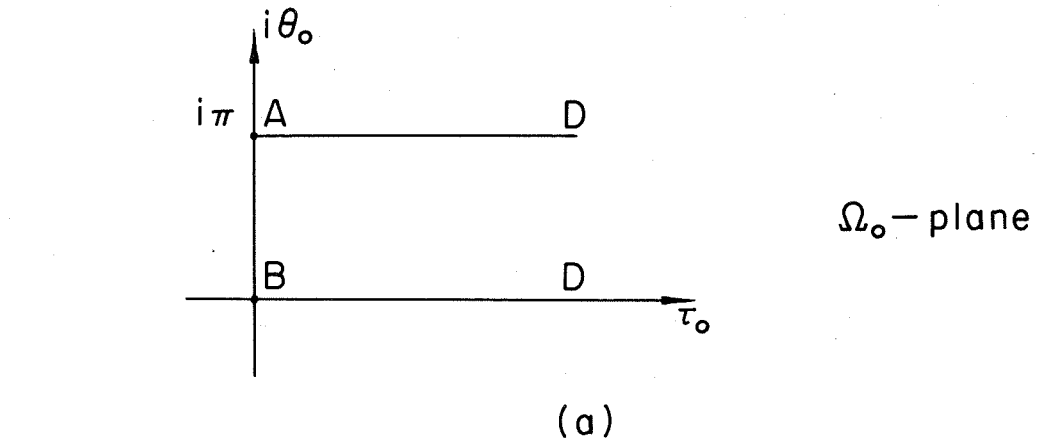

(a)

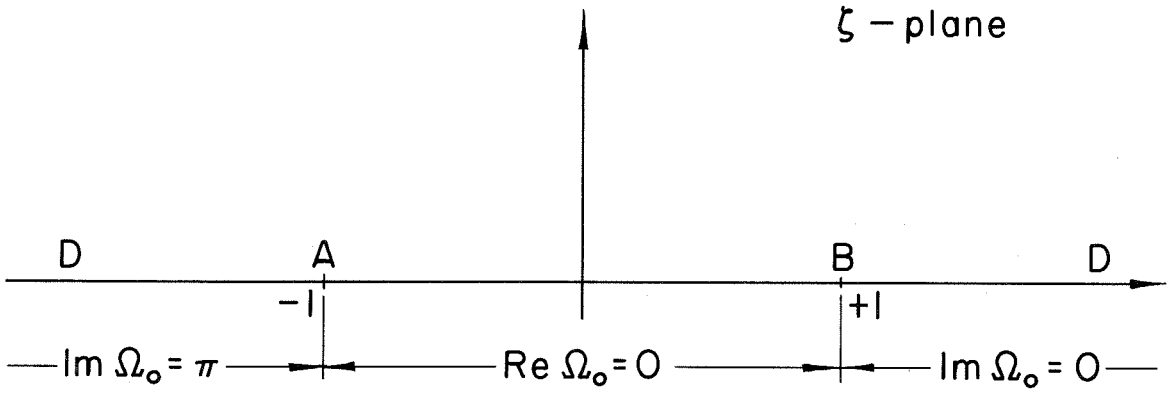

(b)

Fig. 4 The Ω_o- and ζ-planes. $\Omega_o = \cosh^{-1}\zeta = \log(\zeta + \sqrt{\zeta^2 - 1})$.

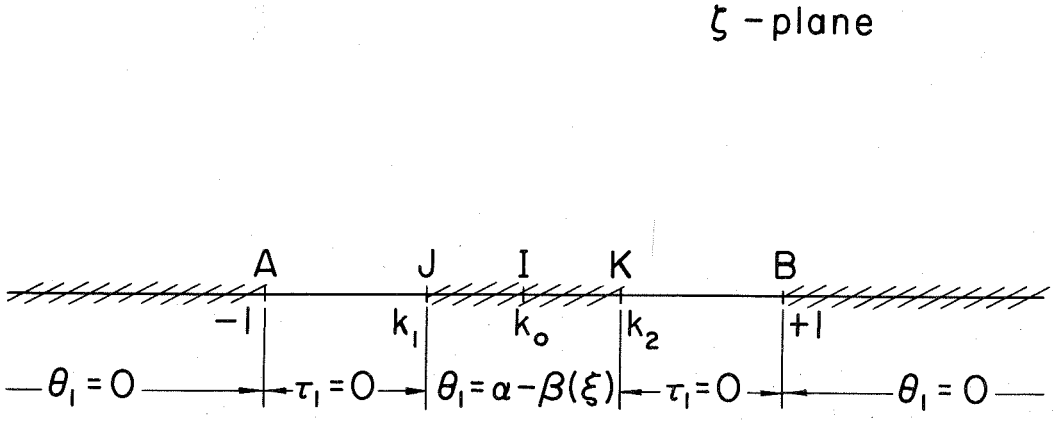

Fig. 5 Boundary values of Ω_1 on Re ζ-axis.

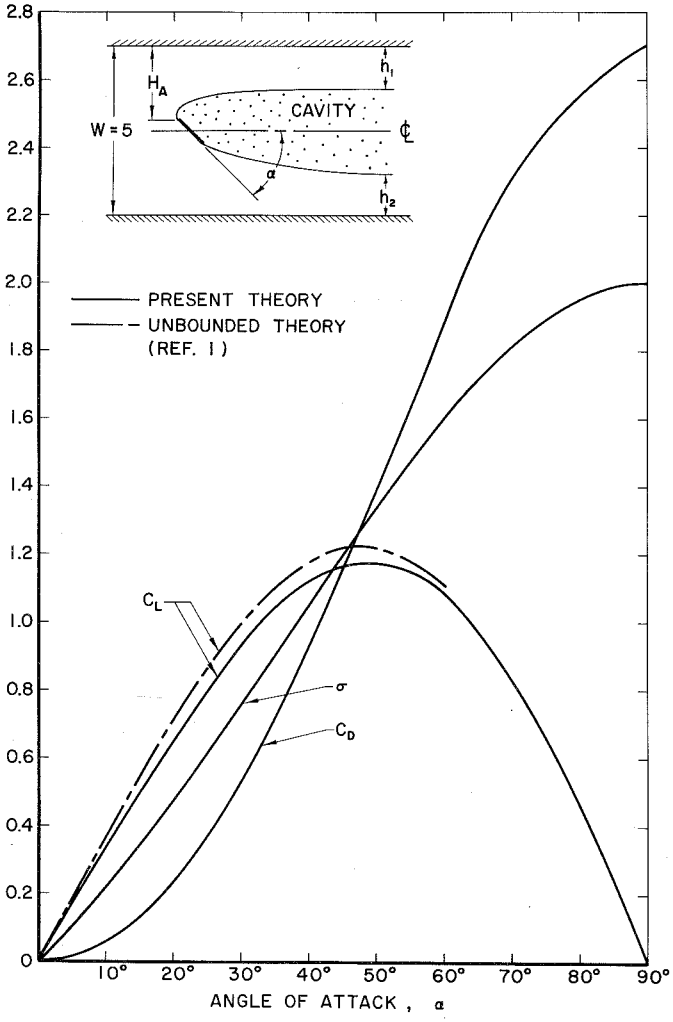

Fig. 6 The dependence of C_L, C_D and σ on the angle of attack, α, for a flat plate located midway in a channel of width W = 5.

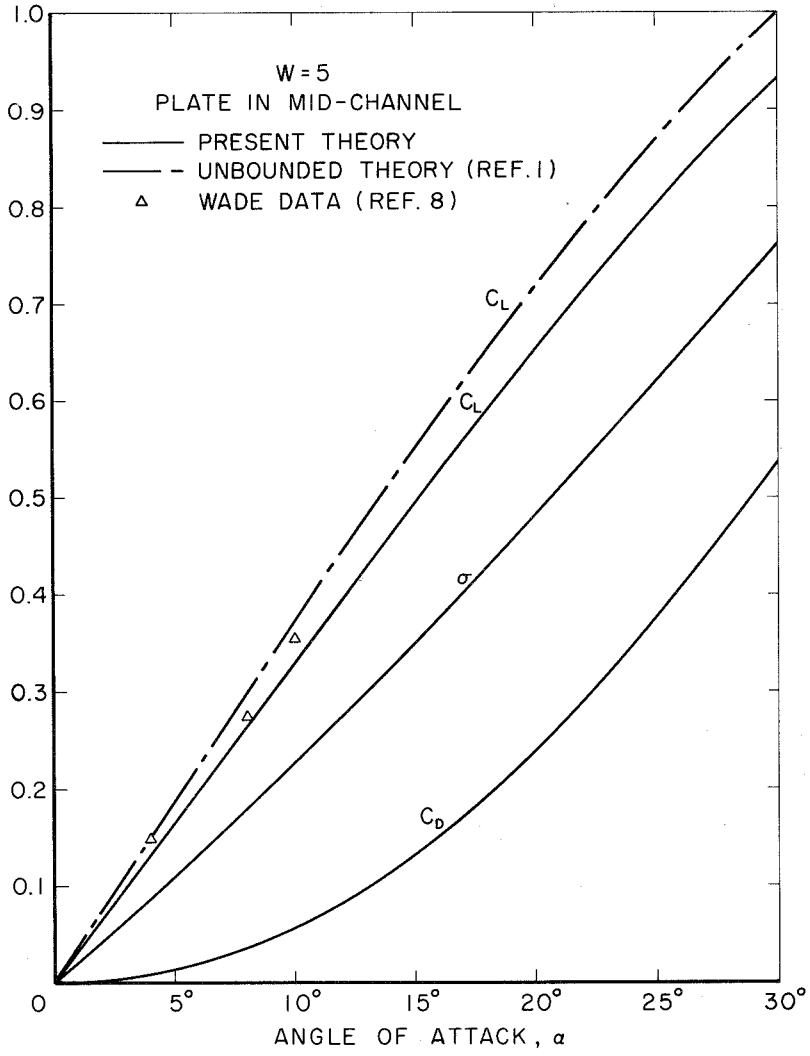

Fig. 7 Enlarged section of Fig 6 for small angles of attack with experimental data extrapolated from Wade's data curves.

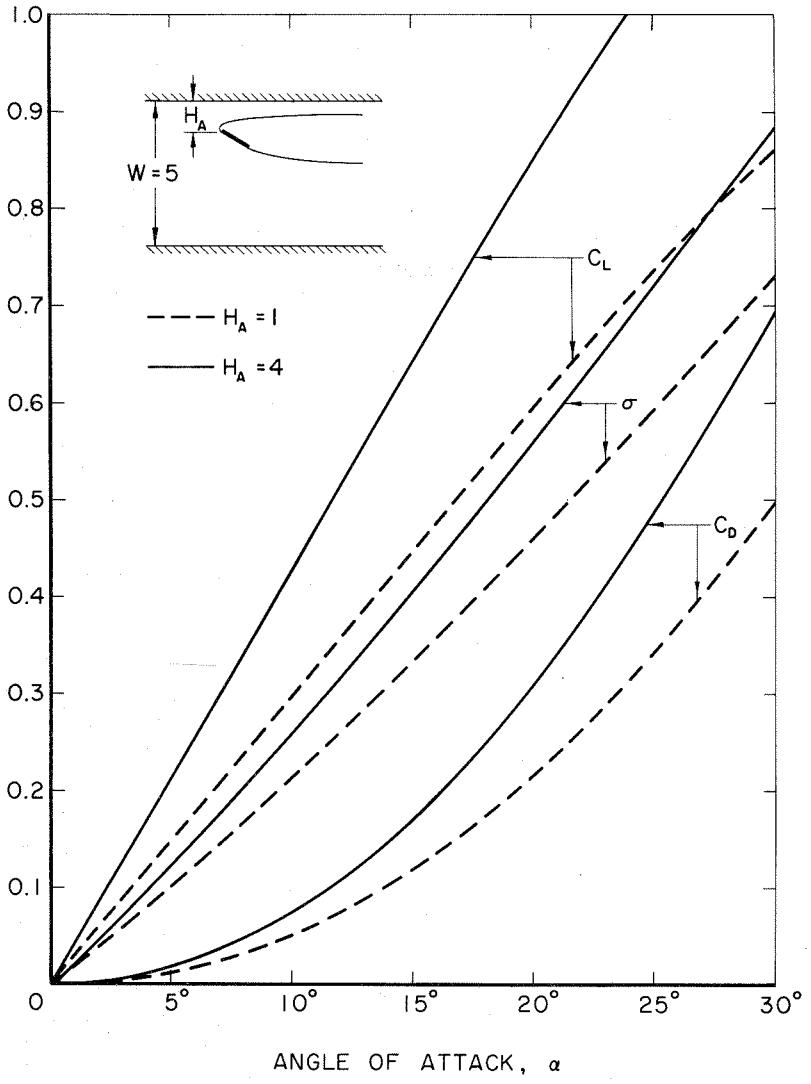

Fig. 8 The effect of angle of attack on C_L, C_D and σ for a flat plate located in two off-center positions in a channel of W = 5.

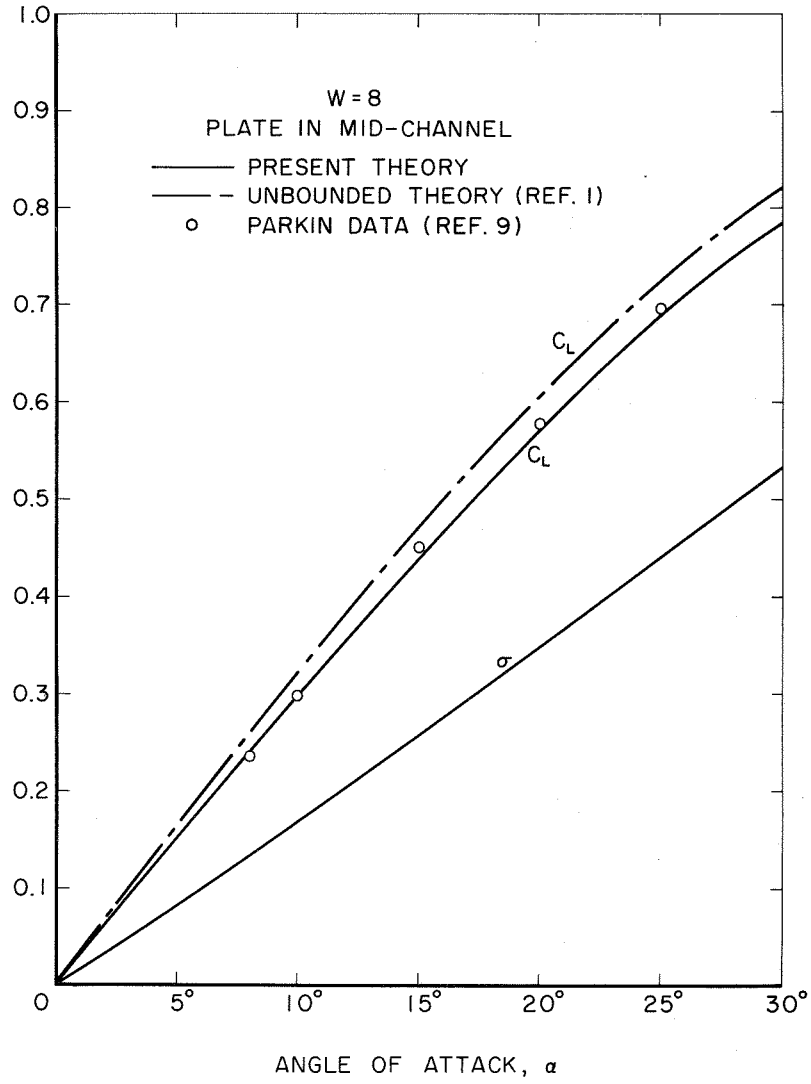

Fig. 9 Comparison of C_L from the present theory with the unbounded theory and experimental data from Parkin for a plate located mid-channel in a channel of W = 8.

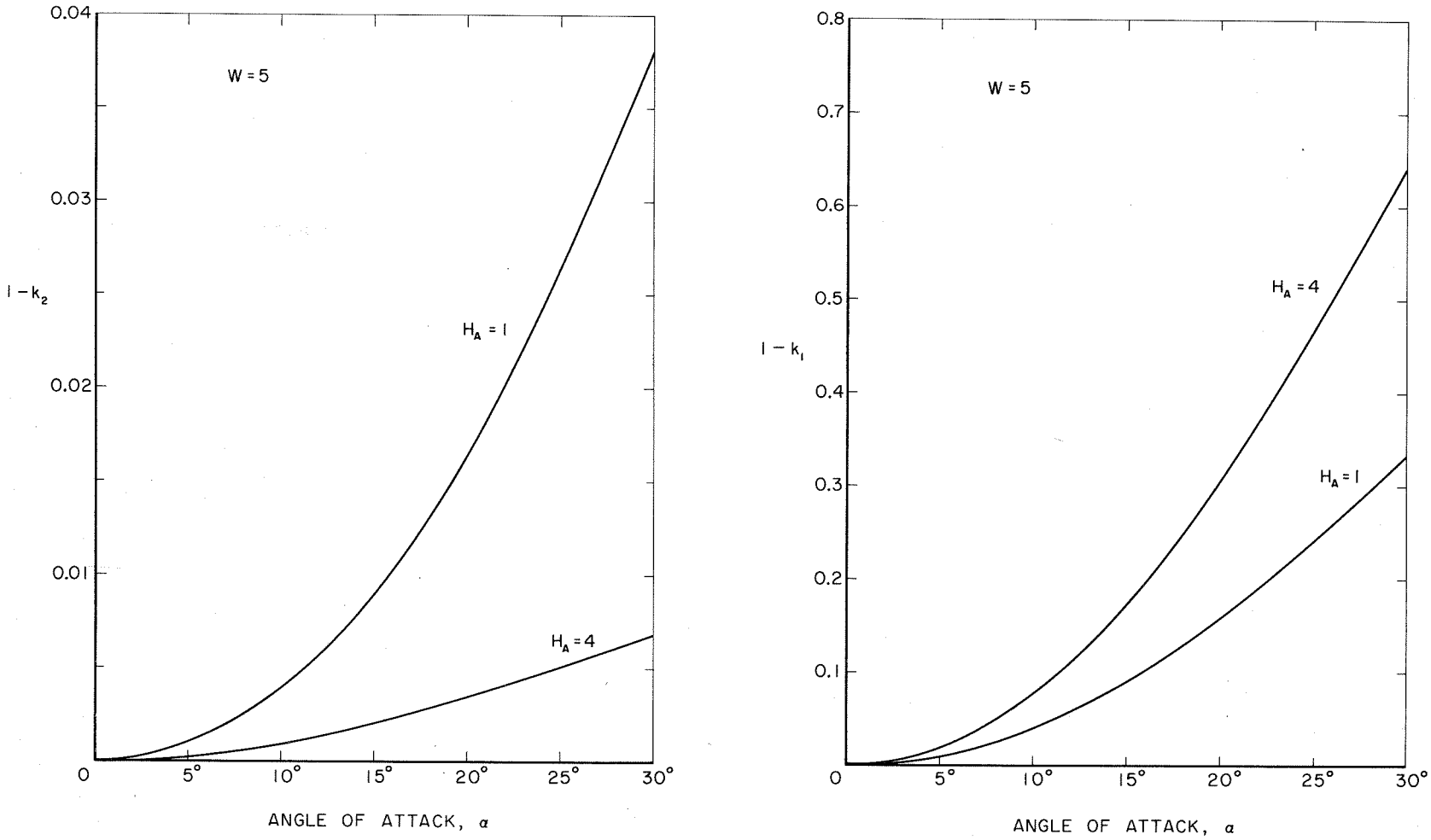

Fig. 10 Effect of channel width on (a) the drag coefficient and (b) the choking cavitation number for a flat plate located mid-channel at various angles of attack.

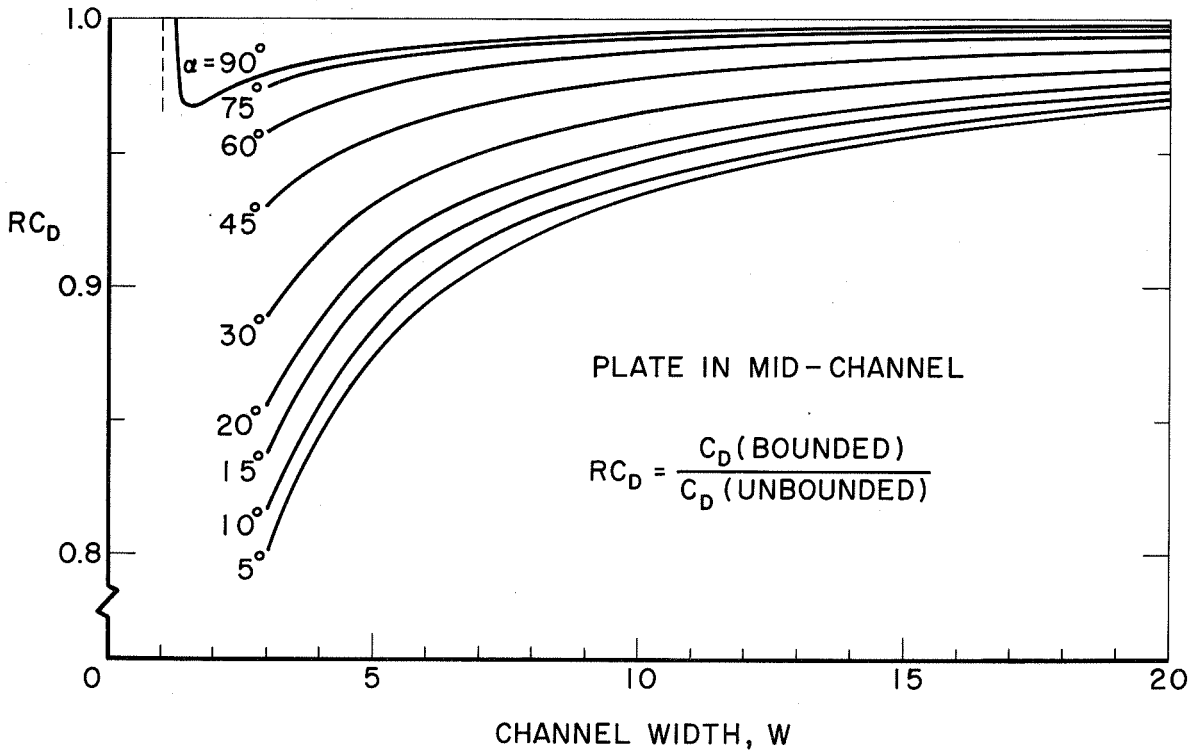

Fig. 11 The ratio of C_D (bounded) to C_D (unbounded) versus W for a flat plate located mid-channel.

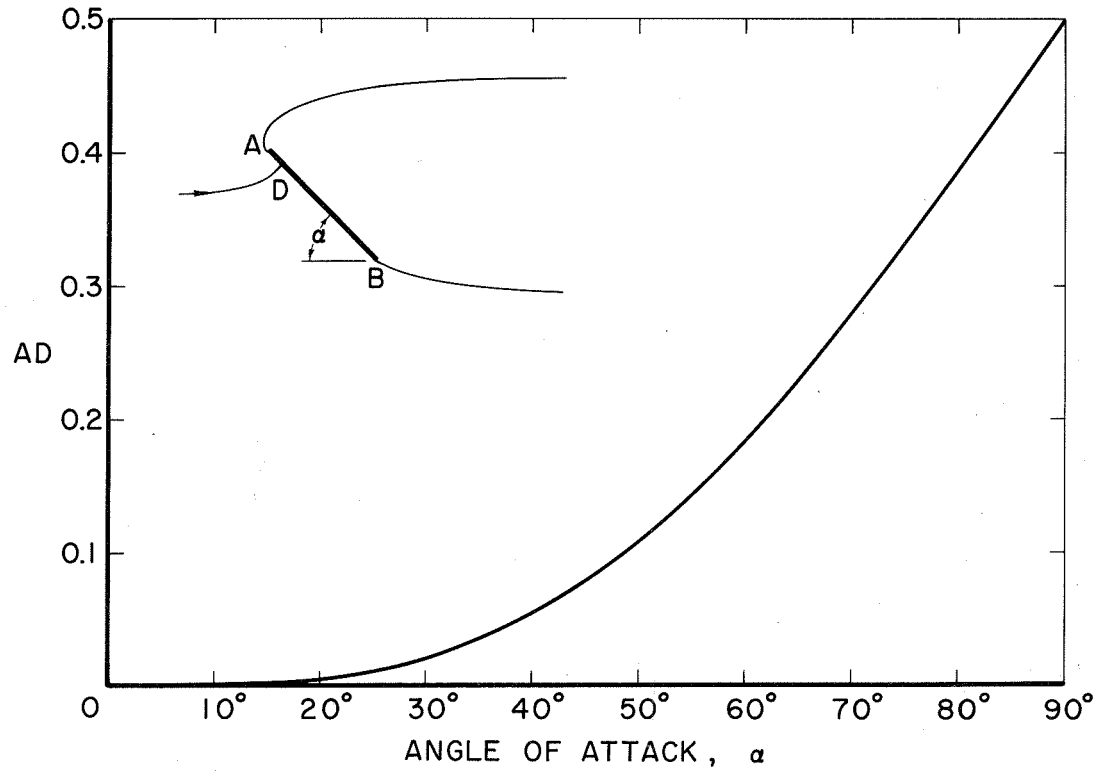

Fig. 12 Distance of stagnation point from the leading edge for W = 5 and the plate in mid-channel.

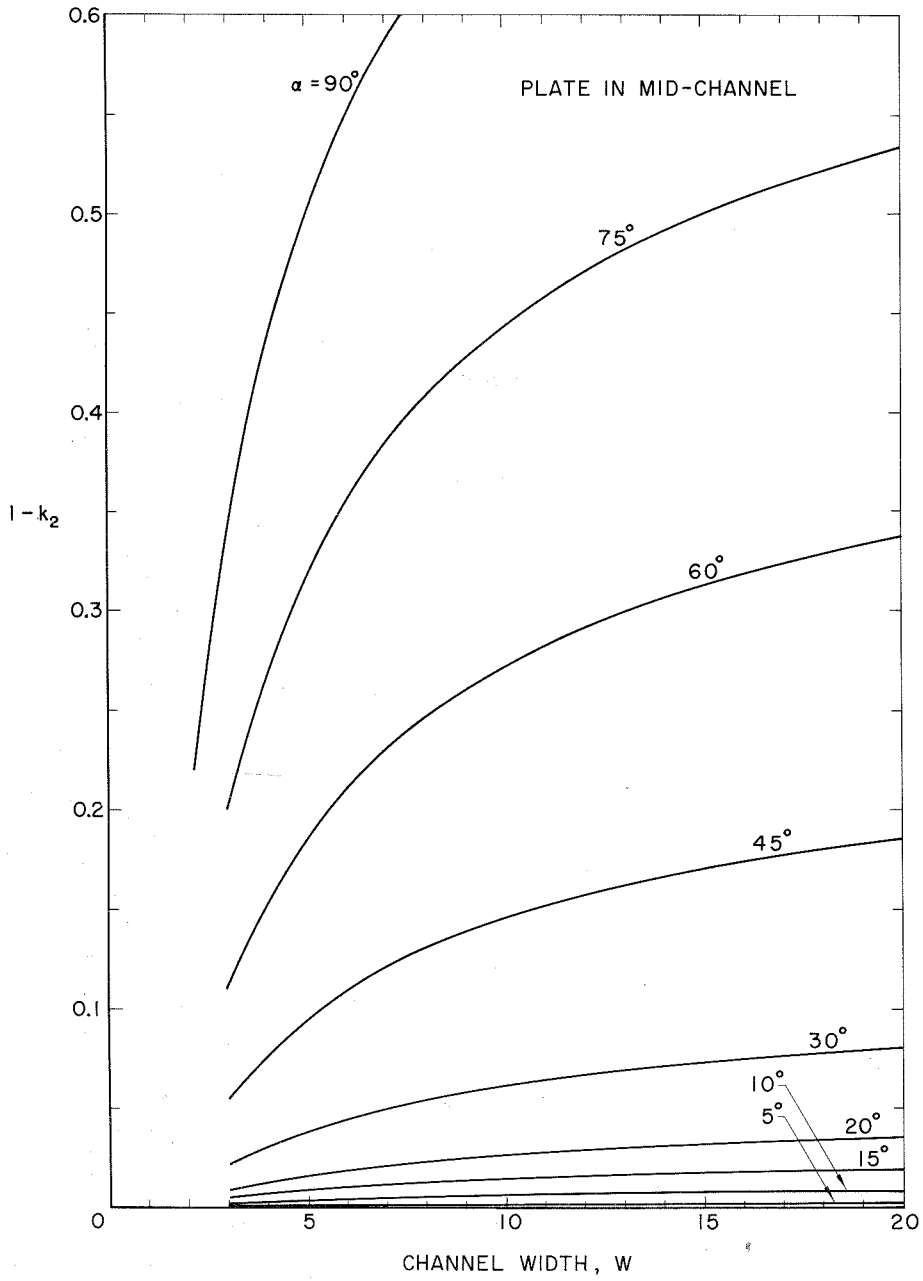

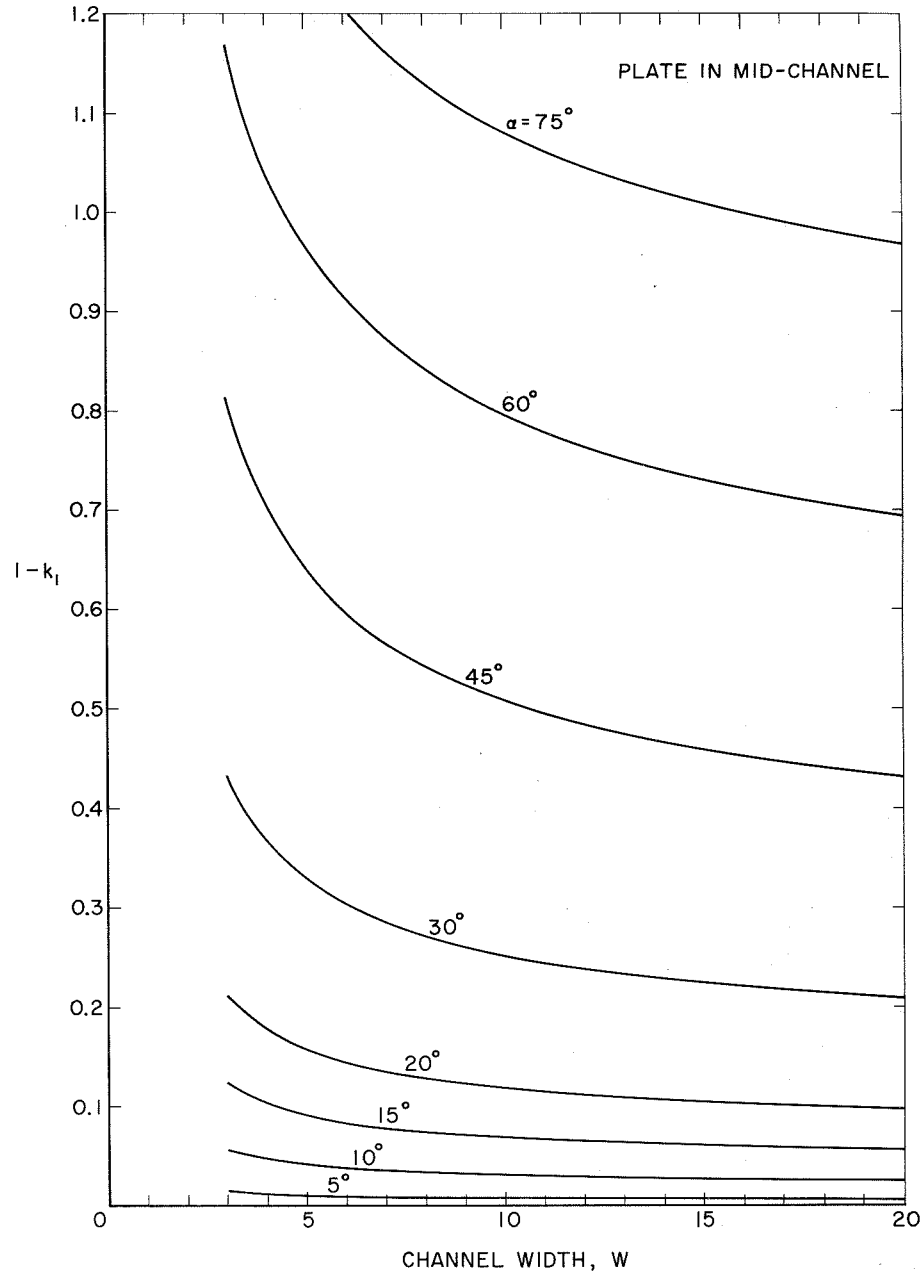

Fig. A-1 Effect of channel width and angle of attack on the transformation parameters (a) k_2 and (b) k_1 for a flat plate located mid-channel.

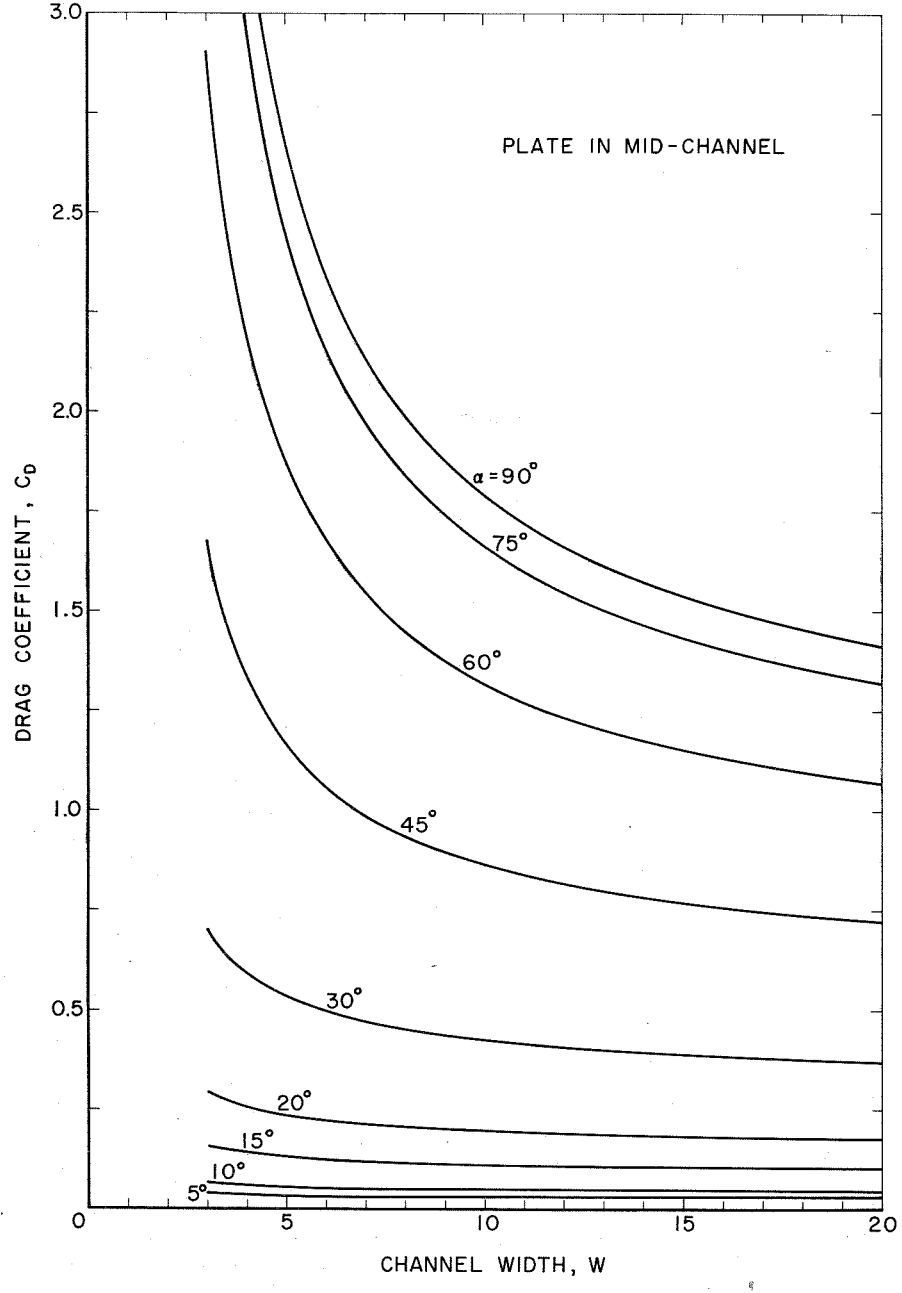

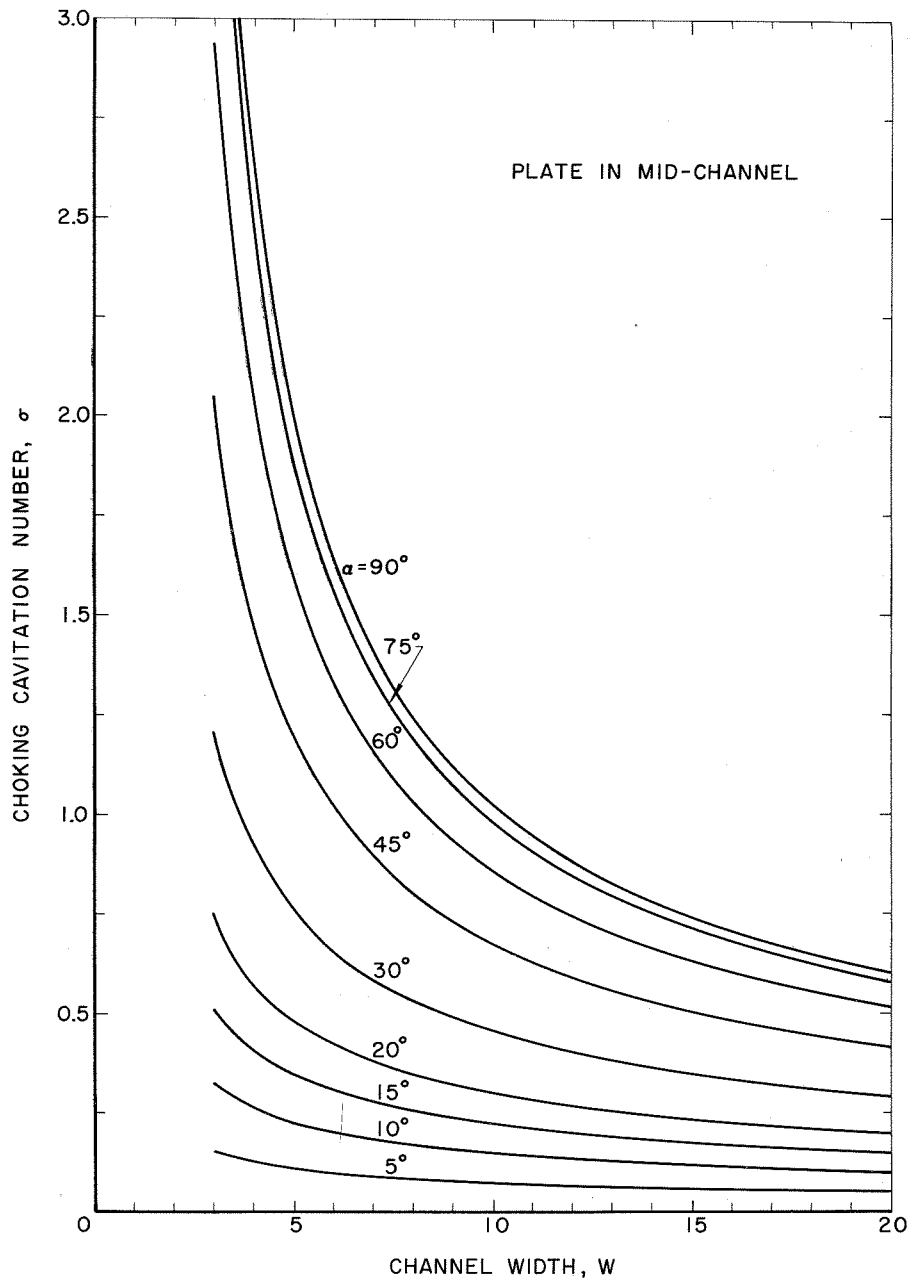

Fig. A-2 Effect of angle of attack and plate position on the transformation parameters (a) k_2 and (b) k_1 for a flat plate in two off-center positions $H_A = 1$ and 4, in a channel of W = 5.

END of Report

DISTRIBUTION LIST FOR UNCLASSIFIED TECHNICAL REPORTS
ISSUED UNDER
CONTRACT Nonr-220(41)
(Single copies unless otherwise specified)

Chief of Naval Research
Department of the Navy
Washington 25, D.C.
Attn: Codes 438 (3)
461
463
466

Commanding Officer
Office of Naval Research
Branch Office
495 Summer Street
Boston 10, Massachusetts

Commanding Officer
Office of Naval Research
Branch Office
207 West 24th Street
New York 11, New York

Commanding Officer
Office of Naval Research
Branch Office
1030 East Green Street
Pasadena, California

Commanding Officer
Office of Naval Research
Branch Office
1000 Geary Street
San Francisco 9, California

Commanding Officer
Office of Naval Research
Branch Office
Box 39, Navy No. 100
Fleet Post Office
New York, New York (25)

Director
Naval Research Laboratory
Washington 25, D. C.
Attn: Code 2027 (6)

Chief, Bureau of Naval Weapons
Department of the Navy
Washington 25, D. C.
Attn: Codes RUAW-r
RRRE
RAAD
RAAD-222
DIS-42

Commander
U. S. Naval Ordnance Test Station
China Lake, California
Attn: Code 753

Chief, Bureau of Ships
Department of the Navy
Washington 25, D. C.
Attn: Codes 310
312
335
420
421
440
442
449

Chief, Bureau of Yards and Docks
Department of the Navy
Washington 25, D. C.
Attn: Code D-400

Commanding Officer and Director
David Taylor Model Basin
Washington 7, D. C.
Attn: Codes 108
142
500
513
520
525
526
526A
530
533
580
585
589
591
591A
700

Commander
U.S. Naval Ordnance Test Station
Pasadena Annex
3202 E. Foothill Blvd.
Pasadena 8, California
Attn: Code P-508

Commander
Planning Department
Portsmouth Naval Shipyard
Portsmouth, New Hampshire

Commander
Planning Department
Boston Naval Shipyard
Boston 29, Massachusetts

Commander
Planning Department
Pearl Harbor Naval Shipyard
Navy No. 128, Fleet Post Office
San Francisco, California

Commander
Planning Department
San Francisco Naval Shipyard
San Francisco 24, California

Commander
Planning Department
Mare Island Naval Shipyard
Vallejo, California

Commander
Planning Department
New York Naval Shipyard
Brooklyn 1, New York

Commander
Planning Department
Puget Sound Naval Shipyard
Bremerton, Washington

Commander
Planning Department
Philadelphia Naval Shipyard
U. S. Naval Base
Philadelphia 12, Pennsylvania

Commander
Planning Department
Norfolk Naval Shipyard
Portsmouth, Virginia

Commander
Planning Department
Charleston Naval Shipyard
U. S. Naval Base
Charleston, South Carolina

Commander
Planning Department
Long Beach Naval Shipyard
Long Beach 2, California

Commander
Planning Department
U. S. Naval Weapons Laboratory
Dahlgren, Virginia

Commander
U. S. Naval Ordnance Laboratory
White Oak, Maryland

Dr. A. V. Hershey
Computation and Exterior
Ballistics Laboratory
U. S. Naval Weapons Laboratory
Dahlgren, Virginia

Superintendent
U. S. Naval Academy
Annapolis, Maryland
Attn: Library

Superintendent
U. S. Naval Postgraduate School
Monterey, California

Commandant
U. S. Coast Guard
1300 E. Street, N. W.
Washington, D. C.

Secretary Ship Structure Committee
U. S. Coast Guard Headquarters
1300 E Street, N. W.
Washington, D. C.

Commander
Military Sea Transportation Service
Department of the Navy
Washington 25, D. C.

U. S. Maritime Administration
GAO Building
441 G Street, N. W.
Washington, D. C.
Attn: Division of Ship Design
Division of Research

Superintendent
U. S. Merchant Marine Academy
Kings Point, Long Island, New York
Attn: Capt. L. S. McCready
(Dept. of Engineering)

Commanding Officer and Director
U. S. Navy Mine Defense Laboratory
Panama City, Florida

Commanding Officer
NROTC and Naval Administrative
Massachusetts Institute of Technology
Cambridge 39, Massachusetts

U. S. Army Transportation Research and
Development Command
Fort Eustis, Virginia
Attn: Marine Transport Division

Mr. J. B. Parkinson
National Aeronautics and Space
Administration
1512 H Street, N. W.
Washington 25, D. C.

Director
Langley Research Center
Langley Station
Hampton, Virginia
Attn: Mr. I. E. Garrick
Mr. D. J. Marten

Director Engineering Sciences Division
National Science Foundation
1951 Constitution Avenue, N. W.
Washington 25, D. C.

Director
National Bureau of Standards
Washington 25, D. C.
Attn: Fluid Mechanics Division
(Dr. G. B. Schubauer)
Dr. G. H. Keulegan
Dr. J. M. Franklin

Defense Documentation Center
Cameron Station
Alexandria, Virginia (20)

Office of Technical Services
Department of Commerce
Washington 25, D. C.

California Institute of Technology
Pasadena 4, California
Attn: Professor M. S. Plesset
Professor T. Y. Wu
Professor A. J. Acosta

University of California
Department of Engineering
Los Angeles 24, California
Attn: Dr. A. Powell

Director
Scripps Institute of Oceanography
University of California
La Jolla, California

Professor M. L. Albertson
Department of Civil Engineering
Colorado A and M College
Fort Collins, Colorado

Professor J. E. Cermak
Department of Civil Engineering
Colorado State University
Fort Collins, Colorado

Professor W. R. Sears
Graduate School of Aeronautical Engineering
Cornell University
Ithaca, New York

State University of Iowa
Iowa Institute of Hydraulic Research
Iowa City, Iowa
Attn: Dr. H. Rouse
Dr. L. Landweber

Massachusetts Institute of Technology
Cambridge 39, Massachusetts
Attn: Department of Naval Architecture
and Marine Engineering
Professor A. T. Ippen

Harvard University
Cambridge 38, Massachusetts
Attn: Professor G. Birkhoff
(Dept. of Mathematics)
Professor G. F. Carrier
(Dept. of Mathematics)

University of Michigan
Ann Arbor, Michigan
Attn: Professor R. B. Couch
(Dept. of Naval Architecture)
Professor W. W. Willmarth
(Aero. Engineering Department)

Dr. L. G. Straub, Director
St. Anthony Falls Hydraulic Laboratory
University of Minnesota
Minneapolis 14, Minnesota
Attn: Mr. J. N. Wetzel
Professor B. Silberman

Professor J. J. Foody
Engineering Department
New York State University Maritime College
Fort Schulyer, New York

New York University
Institute of Mathematical Sciences
25 Waverly Place
New York 3, New York
Attn: Professor J. Keller
Professor J. J. Stoker

The Johns Hopkins University
Department of Mechanical Engineering
Baltimore 18, Maryland
Attn: Professor S. Corrsin
Professor O. M. Phillips (2)

Massachusetts Institute of Technology
Department of Naval Architecture and
Marine Engineering
Cambridge 39, Massachusetts
Attn: Professor M. A. Abkowitz, Head

Dr. G. F. Wislicenus
Ordnance Research Laboratory
Pennsylvania State University
University Park, Pennsylvania
Attn: Dr. M. Sevik

Professor R. C. DiPrima
Department of Mathematics
Rensselaer Polytechnic Institute
Troy, New York

Director
Woods Hole Oceanographic Institute
Woods Hole, Massachusetts

Stevens Institute of Technology
Davidson Laboratory
Castle Point Station
Hoboken, New Jersey
Attn: Mr. D. Savitsky
Mr. J. P. Breslin
Mr. C. J. Henry
Mr. S. Tsakonas

Webb Institute of Naval Architecture
Crescent Beach Road
Glen Cove, New York
Attn: Professor E. V. Lewis
Technical Library

Executive Director
Air Force Office of Scientific Research
Washington 25, D. C.
Attn: Mechanics Branch

Commander
Wright Air Development Division
Aircraft Laboratory
Wright-Pattern Air Force Base, Ohio
Attn: Mr. W. Mykytow, Dynamics Branch

Cornell Aeronautical Laboratory
4455 Genesee Street
Buffalo, New York
Attn: Mr. W. Targoff
Mr. R. White

Massachusetts Institute of Technology
Fluid Dynamics Research Laboratory
Cambridge 39, Massachusetts
Attn: Professor H. Ashley
Professor M. Landahl
Professor J. Dugundji

Hamburgische Schiffbau-Versuchsanstalt
Bramfelder Strasse 164
Hamburg 33, Germany
Attn: Dr. H. Schwanecke
Dr. H. W. Lerbs

Institut fur Schiffbau der
Universitat Hamburg
Berliner Tor 21
Hamburg 1, Germany
Attn: Prof. G. P. Weinblum,

Transportation Technical Research Institute
1-1057, Mejiro-Cho, Toshima-Ku
Tokyo, Japan

Max-Planck Institut fur Stromungsforschung
Bottingerstrasse 6/8
Gottingen, Germany
Attn: Dr. H. Reichardt

Hydro-og Aerodynamisk Laboratorium
Lyngby, Denmark
Attn: Professor Carl Prohaska

Shipsmodelltanken
Trondheim, Norway
Attn: Professor J. K. Lunde

Versuchsanstalt fur Wasserbau and
Schiffbau
Schleuseninsel im Tiergarten
Berlin, Germany
Attn: Dr. S. Schuster, Director
Dr. Grosse

Technische Hogeschool
Institut voor Toegepaste Wiskunde
Julianalaan 132
Delft, Netherlands
Attn: Professor R. Timman

Bureau D'Analyse et de Recherche
Appliquees
47 Avenue Victor Bresson
Issy-Les-Moulineaux
Seine, France
Attn: Professor Siestrunck

Netherlands Ship Model Basin
Wageningen, The Netherlands
Attn: Dr. Ir. J. D. vanManen

National Physical Laboratory
Teddington, Middlesex, England
Attn: Mr. A. Silverleaf, Superintendent
Ship Division
Head, Aerodynamics Division

Head, Aerodynamics Department
Royal Aircraft Establishment
Farnborough, Hants, England
Attn: Mr. M. O. W. Wolfe

Dr. S. F. Hoerner
148 Busteed Drive
Midland Park, New Jersey

Boeing Airplane Company
Seattle Division
Seattle, Washington
Attn: Mr. M. J. Turner

Electric Boat Division
General Dynamics Corporation
Groton, Connecticut
Attn: Mr. Robert McCandliss

General Applied Sciences Labs., Inc.
Merrick and Stewart Avenues
Westbury, Long Island, New York

Gibbs and Cox, Inc.
21 West Street
New York, New York

Lockheed Aircraft Corporation
Missiles and Space Division
Palo Alto, California
Attn: R. W. Kermeen

Grumman Aircraft Engineering Corp.
Bethpage, Long Island, New York
Attn: Mr. E. Baird
Mr. E. Bower
Mr. W. P. Carl

Midwest Research Institute
425 Volker Blvd.
Kansas City 10, Missouri
Attn: Mr. Zeydel

Director, Department of Mechanical Sciences
Southwest Research Institute
8500 Culebra Road
San Antonio 6, Texas
Attn: Dr. H. N. Abramson
Mr. G. Ransleben
Editor, Applied Mechanics Review

Convair
A Division of General Dynamics
San Diego, California
Attn: Mr. R. H. Oversmith
Mr. H. T. Brooke

Hughes Tool Company
Aircraft Division
Culver City, California
Attn: Mr. M. S. Harned

Hydronautics, Incorporated
Pindell School Road
Howard County
Laurel, Maryland
Attn: Mr. Phillip Eisenberg

Rand Development Corporation
13600 Deise Avenue
Cleveland 10, Ohio
Attn: Dr. A. S. Iberall

U. S. Rubber Company
Research and Development Department
Wayne, New Jersey
Attn: Mr. L. M. White

Technical Research Group, Inc.
Route 110
Melville, New York, 11749
Attn: Mr. Jack Kotik

Mr. C. Wigley
Flat 102
6-9 Charterhouse Square
London, E. C. 1, England

AVCO Corporation
Lycoming Division
1701 K Street, N. W.
Apt. No. 904
Washington, D. C.
Attn: Mr. T. A. Duncan

Mr. J. G. Baker
Baker Manufacturing Company
Evansville, Wisconsin

Curtiss-Wright Corporation Research Division
Turbomachinery Division
Quehanna, Pennsylvania
Attn: Mr. George H. Pedersen

Dr. Blaine R. Parkin
AiResearch Manufacturing Corporation
9851-9951 Sepulveda Boulevard
Los Angeles 45, California

The Boeing Company
Aero-Space Division
Seattle 24, Washington
Attn: Mr. R. E. Bateman
(Internal Mail Station 46-74)

Lockheed Aircraft Corporation
California Division
Hydrodynamics Research
Burbank, California
Attn: Mr. Bill East

National Research Council
Montreal Road
Ottawa 2, Canada
Attn: Mr. E. S. Turner

The Rand Corporation
1700 Main Street
Santa Monica, California
Attn: Technical Library

Stanford University
Department of Civil Engineering
Stanford, California
Attn: Dr. Byrne Perry
Dr. E. Y. Hsu

Dr. Hirsh Cohen
IBM Research Center
P. O. Box 218
Yorktown Heights, New York

Mr. David Wellinger
Hydrofoil Projects
Radio Corporation of America
Burlington, Massachusetts

Food Machinery Corporation
P. O. Box 367
San Jose, California
Attn: Mr. G. Tedrew

Dr. T. R. Goodman
Oceanics, Inc.
Technical Industrial Park
Plainview, Long Island, New York

Professor Brunelle
Department of Aeronautical Engineering
Princeton University
Princeton, New Jersey

Commanding Officer
Office of Naval Research Branch Office
219 S. Dearborn Street
Chicago 1, Illinois 60604

University of Colorado
Aerospace Engineering Sciences
Boulder, Colorado
Attn: Prof. M. S. Uberoi

The Pennsylvania State University
Dept. of Aeronautical Engineering
Ordnance Research Laboratory
P. O. Box 30
State College, Pennsylvania
Attn: Professor J. William Holl

Institut fur Schiffbau der Universitat Hamburg
Lammersieth 90
2 Hamburg 33, Germany
Attn: Dr. O. Grim

Technische Hogeschool
Laboratorium voor Scheepsbounkunde
Mekelweg 2, Delft, Netherlands
Attn: Professor Ir. J. Gerritsma

Unclassified

Security Classification

DOCUMENT CONTROL DATA - R&D

(Security classification of title, body of abstract and indexing annotation must be entered when the overall report is classified)

1. ORIGINATING ACTIVITY *(Corporate author)*
Office of Naval Research, Dept. of the Navy
Washington, D. C.

2a. REPORT SECURITY CLASSIFICATION
Unclassified

2b GROUP

3. REPORT TITLE

The Wall Effect in Cavity Flow

4. DESCRIPTIVE NOTES *(Type of report and inclusive dates)*
Final

5. AUTHOR(S) *(Last name, first name, initial)*

Ai, Danield K. and Harrison, Zora L.

6. REPORT DATE	7a. TOTAL NO. OF PAGES	7b. NO. OF REFS
April, 1965	20	9

8a. CONTRACT OR GRANT NO.	9a. ORIGINATOR'S REPORT NUMBER(S)
Nonr-220(41) 61260	E-111.3
b. PROJECT NO.	
c.	9b. OTHER REPORT NO(S) *(Any other numbers that may be assigned this report)*
d.	

10. AVAILABILITY/LIMITATION NOTICES

"Qualified requesters may obtain copies of this report from DDC."

11. SUPPLEMENTARY NOTES	12. SPONSORING MILITARY ACTIVITY
	Office of Naval Research Washington, D. C.

13. ABSTRACT

A nonlinear theory for the calculation of the flow field of an oblique flat plate under blockage condition is given using the techniques of integral equations. Numerical results are obtained with the aid of a high speed digital computer for the plate situated mid-channel at values of the angle of attack from 5^{o} to 90^{o} and the channel-width-chord ratio from 3 to 20. Also obtained are results for the plate situated at two different off-center positions for a channel width-chord ratio of 5 and angles of attack less than 30^{o}.

DD FORM 1 JAN 64 1473

Unclassified

Security Classification

14. KEY WORDS	LINK A		LINK B		LINK C	
	ROLE	WT	ROLE	WT	ROLE	WT

INSTRUCTIONS

1. ORIGINATING ACTIVITY: Enter the name and address of the contractor, subcontractor, grantee, Department of Defense activity or other organization *(corporate author)* issuing the report.

2a. REPORT SECURITY CLASSIFICATION: Enter the overall security classification of the report. Indicate whether "Restricted Data" is included. Marking is to be in accordance with appropriate security regulations.

2b. GROUP: Automatic downgrading is specified in DoD Directive 5200.10 and Armed Forces Industrial Manual. Enter the group number. Also, when applicable, show that optional markings have been used for Group 3 and Group 4 as authorized.

3. REPORT TITLE: Enter the complete report title in all capital letters. Titles in all cases should be unclassified. If a meaningful title cannot be selected without classification, show title classification in all capitals in parenthesis immediately following the title.

4. DESCRIPTIVE NOTES: If appropriate, enter the type of report, e.g., interim, progress, summary, annual, or final. Give the inclusive dates when a specific reporting period is covered.

5. AUTHOR(S): Enter the name(s) of author(s) as shown on or in the report. Enter last name, first name, middle initial. If military, show rank and branch of service. The name of the principal author is an absolute minimum requirement.

6. REPORT DATE: Enter the date of the report as day, month, year, or month, year. If more than one date appears on the report, use date of publication.

7a. TOTAL NUMBER OF PAGES: The total page count should follow normal pagination procedures, i.e., enter the number of pages containing information.

7b. NUMBER OF REFERENCES: Enter the total number of references cited in the report.

8a. CONTRACT OR GRANT NUMBER: If appropriate, enter the applicable number of the contract or grant under which the report was written.

8b, 8c, & 8d. PROJECT NUMBER: Enter the appropriate military department identification, such as project number, subproject number, system numbers, task number, etc.

9a. ORIGINATOR'S REPORT NUMBER(S): Enter the official report number by which the document will be identified and controlled by the originating activity. This number must be unique to this report.

9b. OTHER REPORT NUMBER(S): If the report has been assigned any other report numbers *(either by the originator or by the sponsor)*, also enter this number(s).

10. AVAILABILITY/LIMITATION NOTICES: Enter any limitations on further dissemination of the report, other than those imposed by security classification, using standard statements such as:

(1) "Qualified requesters may obtain copies of this report from DDC."

(2) "Foreign announcement and dissemination of this report by DDC is not authorized."

(3) "U. S. Government agencies may obtain copies of this report directly from DDC. Other qualified DDC users shall request through _____."

(4) "U. S. military agencies may obtain copies of this report directly from DDC. Other qualified users shall request through _____."

(5) "All distribution of this report is controlled. Qualified DDC users shall request through _____."

If the report has been furnished to the Office of Technical Services, Department of Commerce, for sale to the public, indicate this fact and enter the price, if known.

11. SUPPLEMENTARY NOTES: Use for additional explanatory notes.

12. SPONSORING MILITARY ACTIVITY: Enter the name of the departmental project office or laboratory sponsoring *(paying for)* the research and development. Include address.

13. ABSTRACT: Enter an abstract giving a brief and factual summary of the document indicative of the report, even though it may also appear elsewhere in the body of the technical report. If additional space is required, a continuation sheet shall be attached.

It is highly desirable that the abstract of classified reports be unclassified. Each paragraph of the abstract shall end with an indication of the military security classification of the information in the paragraph, represented as *(TS)*, *(S)*, *(C)*, or *(U)*.

There is no limitation on the length of the abstract. However, the suggested length is from 150 to 225 words.

14. KEY WORDS: Key words are technically meaningful terms or short phrases that characterize a report and may be used as index entries for cataloging the report. Key words must be selected so that no security classification is required. Identifiers, such as equipment model designation, trade name, military project code name, geographic location, may be used as key words but will be followed by an indication of technical context. The assignment of links, rules, and weights is optional.